气动激励装置原型机磁共振弹性成像研究

黄文慧 蔡葳蕤 邹 超 曾成志 钟耀祖 张丽娟 郑海荣

（ 中国科学院深圳先进技术研究院 深圳 518055 ）

摘 要 介绍：磁共振弹性成像是一种无创的对生物组织的生物力学特性进行定量分析的新技术。在诸多外部机械激励方法中，气动激励装置因其磁兼容性好而相对被广泛使用。本研究搭建了一台气动装置原型机并测试了该装置在不同频率和振幅条件下的性能。材料和方法：使用超声方法测试气动激励装置原型机在无负载条件和不同频率和振幅情况下的性能，并在磁共振弹性成像环境测试该原型机在有负载条件下的性能。结果：生物组织的弹性值与外部激励的频率和振幅、生物组织的机械力学特性以及传导管的长度和内径有关。结论：稳定可靠的机械波是磁共振弹性成像中准确可靠地重建组织弹性值的保障，气动激励装置的机械激励参数应根据不同生物组织的特性进行优化，以保证弹性值重建的可靠性。

MR Elastography with A Prototype Pneumatic Driver

HUANG Wen-hui CAI Wei-rui ZOU Chao ZENG Cheng-zhi CHUNG Yiu-cho

ZHANG Li-juan ZHENG Hai-rong

(*Shenzhen Institutes of Advanced Technology, Chinese Academy of Sciences, Shenzhen* 518055, *China*)

Abstract Introduction: Magnetic resonance elastography (MRE) is a non-invasive technique to quantitatively assess the mechanical properties of biological tissue. Among multiple actuation methods, pneumatic driver is popularly used due to the advantage of good MR compatibility. In this study we set up a prototype pneumatic driver and investigate its performance under MRE with stimulations of various amplitude-frequency pairs.Materials and Methods: Load-free performance of the driver was tested using ultrasound with stimulations of various amplitude-frequency pairs. Performance with load was tested using MRE with both tissue mimicking phantoms and leg muscle. Results: Frequency and amplitude of the external stimulation, mechanical properties of biological tissue, and the length and the diameter of the transmission tube were all found to affect the elastogram reconstruction. Conclusions: A MR compatible actuating driver generating reliable mechanical stimulation is required to guarantee stable propagating shear waves in tissue. Optimal actuating parameters should be properly determined in the practice of MRE for specific tissue.

1 Introduction

Magnetic resonance elastography (MRE) is a rapidly developing technology for quantitatively assessing the mechanical properties of biological tissue [1-4]. It is a phase-contrast-based imaging technique that can measure propagating acoustic shear waves in tissue subjective to harmonic mechanical excitation and allow for the calculation of local shear modulus that depict tissue elasticity [3], even for deep located tissues such as liver [5]. This technique provides a unique image contrast based on tissue stiffness. MRE has shown promising applications in hepatic fibrosis and sclerosis differentiating[5], brain disease [6], tumor characterization, particularly in breast[7, 8], liver [9, 10], kidney and prostate,

作者简介：黄文慧，研究方向为弹性成像机械激励装置设计、体模制备、成像参数优化以及弹性重建算法等；蔡葳蕤，弹性成像机械激励装置设计、体模制备、成像参数优化以及弹性重建算法等；邹超，高级工程师，研究方向为图像处理和模式识别，数字信号处理和时间序列分析；曾成志，高级工程师，研究方向为超声波束形成、数字信号处理、海量数据传输等关键技术；钟耀祖，博士，研究员，研究方向为磁共振血管壁成像、缺血性心脏病成像与心肌衰弱组织特性的早期；张丽娟，硕士，副研究员，研究方向为中枢神经系统定量磁共振弥散向量成像(DTI)及磁共振波谱(MRS)等技术在大脑发育、外伤、退行性变、脱髓鞘疾病的应用基础研究，磁共振弹性成像（MRE），高分辨低剂量CT早期肺癌筛查等；郑海荣，博士，研究员，研究方向为超声学、超声成像-给药-治疗一体化及多模态医学影像。

and assessment of rehabilitation of muscle [11, 12].

The technique of MRE essentially involves generating acoustic shear wave within tissues via a coupled, MR compatible, mechanical driver, acquiring MR phase images depicting the propagation of the shear waves by a special pulse sequence synchronized with motion sensitive gradients, and calculate tissue stiffness to create MR elastogram map [1, 13, 14].

Achieving adequate signal-to-noise ratio (SNR) for post processing methods of reconstruction of elasticity values from the phase images usually requires a spin displacement on the order of several tens of micrometers within the region of interest[3, 15]. However, there are no generally accepted rules for optimizing the acquisition parameters in various tissues have been established. The optimal values have to be found by performing trial runs for each MRE setup preceding application to a new tissue type, say biceps, brain, or liver, but the parameters do not as a rule have to be optimized in individual subjects [16].

Good performance of the mechanical actuator is essential to provide mechanical wave with steady frequency and sufficient amplitude during image acquisition. Among multiple designs pneumatic actuator is mostly used for its advantages of good MR compatibility, being inexpensive and more practical in clinical applications [9, 17, 18, 19]. However, in a pneumatic system air is intrinsically compressible medium [20], which may complicate the power transfer via a long transmission tube. It is essential to investigate the performance of the pneumatic driver under different excitation parameters with and without load to optimize imaging parameters of an MRE study. To understand the driver's performance, we setup a prototype MR compatible pneumatic driver with frequency bandwidth of 50 Hz-150 Hz in this study. Its load-free performance was tested using ultrasound method, and validated its application with load using tissue mimicking phantom and leg muscle.

2 Materials and Methods

A. The Prototype Pneumatic Driver Setup

The prototype pneumatic driver system consists of a loudspeaker outside the scanning room as active driver to generate air mechanical vibration from 50 Hz to 150 Hz (Fig. 1). The air mechanics is transmitted to a passive driver via a plastic tube which was sealed with a thin membrane at the free end. The membrane vibrates in response to the air vibration and serving as passive driver to induce acoustic shear wave in tissue. An amplified sine signal was applied to excite the loudspeaker and synchronized to the imaging sequence [9, 10].

B. Load free performance experiment

The response of the passive driver membrane to mechanical stimulation under unloading was tested using ultrasound in water. The tube and the passive driver membrane were fixed in a water tank located at the focal spot of an 5 MHz ultrasound transducer which emits RF pulse to the center of the membrane at a pulse repeat frequency (PRF) of 10 KHz. The first reflected pulse was received to calculate the distance between the transducer and the membrane when it vibrated in sine waveform. A Field-Programmable Gate Array (FPGA) module was applied to synchronize the loudspeaker and the signal acquisition as well as the Pulser/Receiver (OLIMPUS 5800). Signal was sampled by ADC (NI PXI-5122) with total memory of 10 M at the frequency of 25 MHz. The

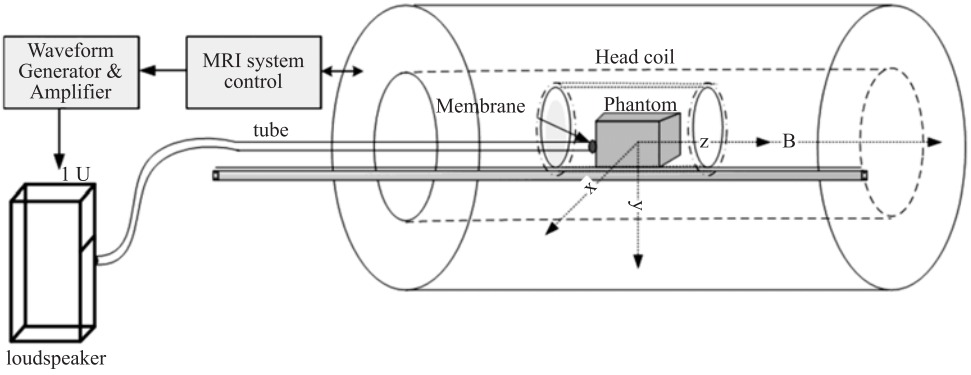

Figure 1. The setup of a prototype pneumatic driver

corresponding acquisition time was 400 ms. Data of the ultrasound RF signal was acquired in two mode:

Mode I: Signal Generator was synchronized with AD data acquisition. The loudspeaker was synchronized with ultrasound transducer and ADC. Time delay and transient response of the membrane vibration were recorded.

Mode II: Signal Generator worked prior to the ultrasound transducer and AD data acquisition for a few seconds. The loudspeaker was turned on before the RF signal. The steady response of the membrane vibration was recorded.

Data processing was performed using MATLAB (R2008a, MathWorks, USA). The derived membrane vibration information were calculated using cross correlation by the first reflect RF pulse with three setups of different tube dimensions and actuating frequencies as summarized in TAB.I. The actuating frequency and Peak voltage output from amplifier varied from 50 Hz to 150 Hz with a 10 Hz step, and 3 V, 6 V, 10 V, 12 V and 15 V, respectively.

C. Phamtom MRE with the Prototype Pneumatic Driver

A homogeneous gel phantom measuring 13.5 cm×13.0 cm ×7.0 cm was fabricated simulating the elasticity of human soft tissue. Another homogeneous phantom of 18 cm×11 cm×6 cm with an embedded firmer gel ball of 4 cm in diameter was fabricated to simulate a tumor.

A 2D MRE gradient echo pulse sequence synchronizing to the external oscillation of the pneumatic driver was executed at a 3.0T MR scanner (Siemens Trio) with a 12 channel head coil. TR and TE varied in correspondence to the frequency of external excitation, as shown in TAB. II. Image matrix was 64 mm×256 mm, FOV was 180 mm×180 mm, imaging plane was coronal, motion sensitive gradient (MSG) was applied at Z-direction. MR scans were repeated along with the mechanical wave of 4 phase offsets (0°, 90°, 180°and 270°) with respect to the MSG to get visualization of wave propagation as a cine loop [21]. All images were acquired after the loudspeaker was turned on for 1 minute to ensure that the acoustic strain waves reached steady state. Phase images were unwrapped using the method described in [22]. MREWAVE software (Mayo clinic) was employed to reconstruct the phantom elastogram using local frequency estimation (LFE) algorithm [23, 24]. The MRE flow chart is shown as Fig. 2.

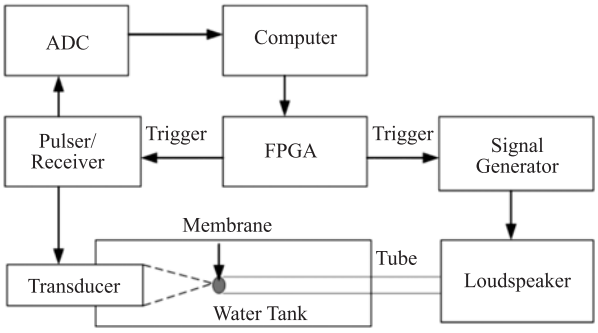

Figure 2. The flow chart of MRE on agar phantom with the prototype pneumatic driver

D. MRE on Human Leg Muscle Using the Prototype Pneumatic Driver

This study was approved by local Institutional Review Board and informed consent was obtained prior to the MRE study for the subject. The passive driver was immobilized respectively under the lower leg and thigh of a healthy 26-year-old male. Stimulation ranged from 60 Hz to 100 Hz in frequency and 10 V~17 V in amplitude. A 2D MRE sequence was applied with a 6 channel surface coil. The Imaging parameters were the same as aforementioned in the phantom study.

3 Results

A. Load Free Performance of the Driver

The load-free vibration response of the passive driver membrane was shown in Fig. 3. Similar responses were observed with 50 Hz~150 Hz with that of 80 Hz with tube I was demonstrated as a representative. Fig. 3a displayed the time delay and transient response under mode I, during which the phase and amplitude changed irregularly. The time delay was due to the air transmission through the long tube. Fig. 3b showed that the response reached a steady state in phase and amplitude under mode II. Steady state was reached from the last 7 cycles in Fig. 3a from which the time for the vibration to reach steady state with tube I from beginning was about 300 ms, for 80 Hz. The delay time varied with actuating frequencies ranging from 50 Hz~150 Hz, from 194 ms to 300 ms.

B. Phantom MRE

Representative phase image and reconstructed elastogram of a homogeneous tissue-like phantom at excitation

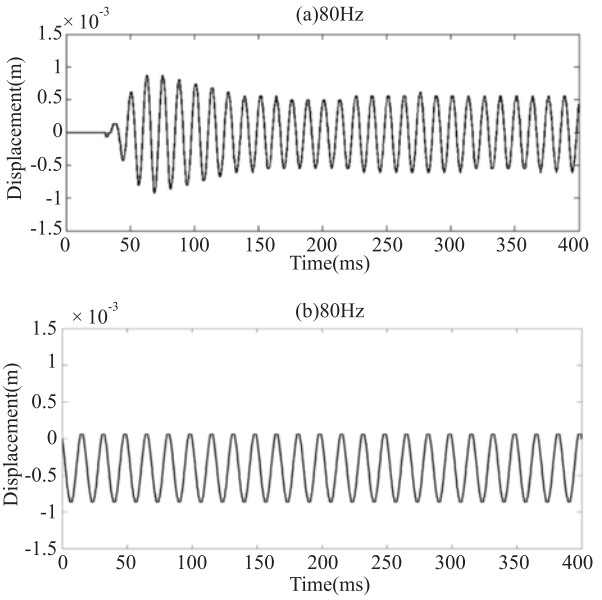

Figure 3. Load free performance experiment of the prototype pneumatic driver. A time delay and transient response under mode I was observed, during which the phase and amplitude of the passive driver changed irregularly (a). Frequency response reached a steady state in phase and amplitude under mode II. Steady state was reached from the last 7 cycles in Fig. 3a, from which the time for the vibration to reach steady state with tube I was about 300 ms (b)

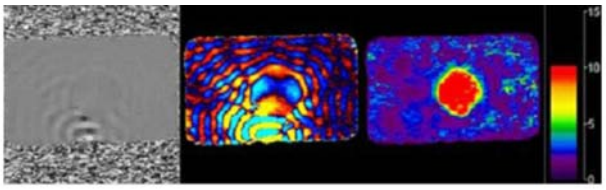

Figure 4. Representative phase image and reconstructed elastogram of a homogeneous tissue-like phantom at excitation frequency of 120 Hz

frequency of 100 Hz/5 v was shown in Fig. 4. Firmer inclusion was clearly distinguished from the surrounding background, and their stiffness was estimated as 2.28 kpa and 11.79 kpa, respectively. Shear modulus estimated under different harmonic mechanical frequencies and amplitude was summarized in TAB. III. At a given frequency, elasticity estimation increased with increasing oscillating amplitude of the actuator (Fig. 5a); with a controlled amplitude and mechanical frequency ranged from 50 Hz to 150 Hz, the elasticity estimate showed a trend of increase followed by a declination (Fig. 5b).

C. MRE on Human Leg Muscle

Representative MRE images and reconstructed elastogram of human lower leg and thigh muscle were shown in Fig. 6. External excitation were 100 Hz/15 v(middle row)and 60 Hz/15 v(bottom row), respectively. MRE of 60 Hz showed better wave propagation and elastogram than that of 100 Hz which induced too little shear wave to evaluate stiffness in bone area.

4 Discussion and Conclusions

This study with MRE setup verified that MRE work well on phantom to visualize the elastogram. Study on the performance of pneumatic driver demonstrated that the vibration of passive driver underwent a time delay and

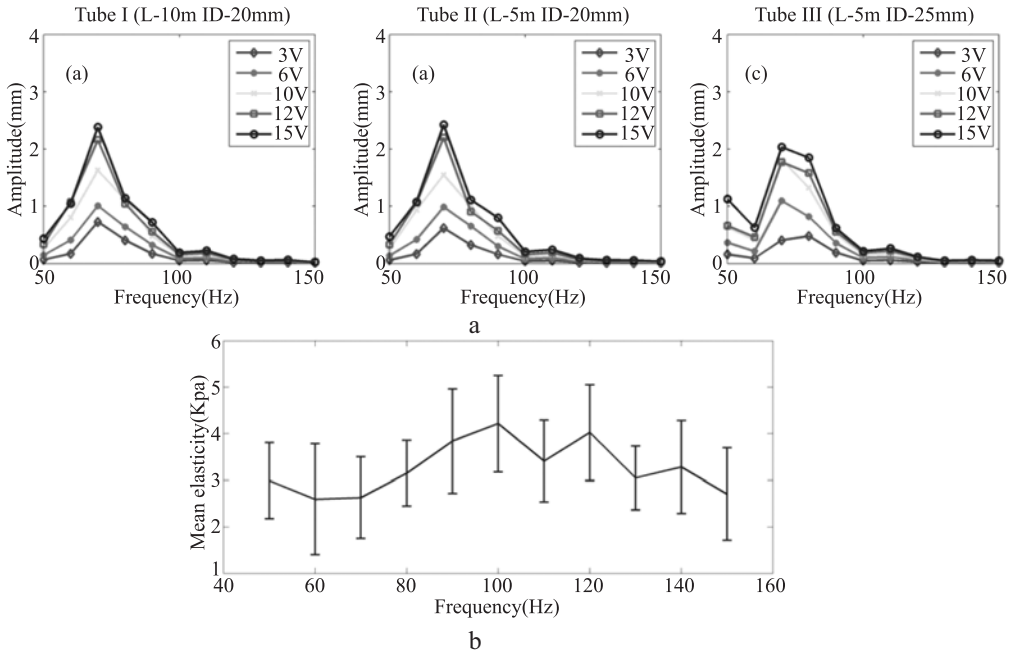

Figure 5. At a given frequency, elasticity estimation increased with increasing oscillating amplitude of the actuator (a); with a controlled amplitude and mechanical frequency ranged from 50 Hz to 150 Hz, the elasticity estimate showed a trend of increase followed by a declination (b)

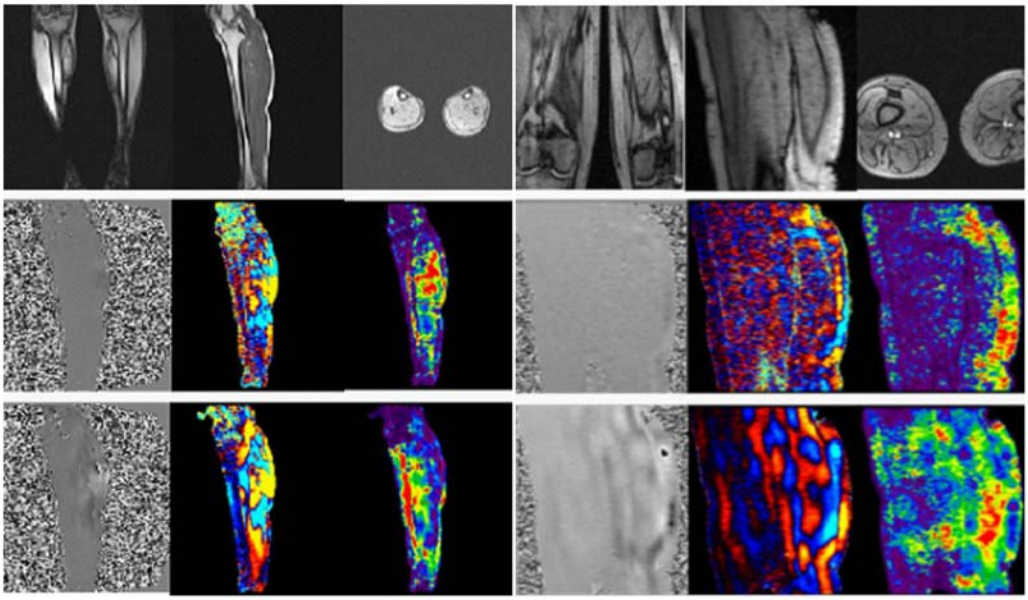

Figure 6. Representative MRE images and reconstructed elastogram of the calf and thigh muscle of a healthy volunteer (27 years, male). External excitations were 100 Hz/15 v(middle row)and 60 Hz/15 v(bottom row), respectively

transient response to reach steady state after excitation. This suggests that a dummy period is needed to ensure an optimal MRE data acquisition. The different vibration amplitude response at steady state to various actuating frequency and input voltage varied with dimensions of transmission tube. This supports the truth that the pneumatic driver has complicated nonlinear properties because of air compressibility. Mechanical stimulation of a pneumatic driver needs to be adjusted properly during MRE study for specific biological tissues with different mechanical properties; the intensity of the mechanical wave propagating in the tissue has great influence on the estimation of elasticity. To achieving adequate signal-to-noise ratio (SNR) for reconstruction of elasticity values from the phase images, this study explained that adequate amplitude of wave propagation in all regions of tissue for image acquisition with sufficient information is a must for accurate reconstruction of tissue elastogram, and intensity is meanly controlled by conditions such as driver excitation frequency and amplitude, structural anisotropy as well as the mechanical properties of the imaged tissue. The estimation of elasticity increased with increasing excitation amplitude of the actuator, and the frequency also has a great influence on estimation of elasticity. So it is crucial to choose optimal parameters of a pneumatic driver in practice to guarantee appropriate shear wave and reliable stiffness estimation of biological tissue.

References

[1] Muthupillai R, Lomas D J, Rossman P J, et al. Magnetic resonance elastography by direct visualization of propagating acoustic strain waves [J]. Science, 1995, 269: 1854-1857.

[2] Muthupillai R, Rossman P J, Lomas D J, et al. Magnetic resonance imaging of transverse acoustic strain waves [J]. Magnetic Resonance in Medicine,1996, 36: 266-274.

[3] Manduca A, Oliphant T E, Dresner M A, et al. Magnetic resonance elastography: non-invasive mapping of tissue Elasticity [J]. Medical Image Analysis, 2001, 5: 237-254.

[4] Mariappan Y K, Glaser K J, Ehman R L. Magnetic resonance elastography: a review [J]. Clinical Anatomy, 2010, 23: 497-511.

[5] Peeters F, Sinkus R, Salameh N, et al. In vivo MR elastography of liver fibrosis [C] // Proceedings of 13th Annual Meeting ofInternational Society for Magnetic Resonance in Medicine, Florida, USA, 2005: 339.

[6] Kruse S A, Dresner M A, Rossman P J, et al. Palpation of the brain using magnetic resonance elastography [C] // Proceedings of 7th Annual Meeting of International Society for Magnetic Resonance in Medicine, Pennsylvania, USA, 1999: 258.

[7] Lawrence A J, Muthupillai R, Rossman P J, et al. MR elastography of the breast: preliminary results [C] // Proceedingsof 6th Annual Meeting ofInternational Society for Magnetic Resonance in Medicine, Sydney, Australia, 1998: 233.

[8] Lawrence A J, Rossman P J, Mahowald J L, et al. Assessment of breast cancer by magnetic resonance elastography [C] // Proceedings of 7th Annual Meeting ofInternational Society for Magnetic Resonance in Medicine, Pennsylvania, USA, 1999: 525.

[9] Dresner M A, Fidler J L, Ehman R L. MR elastography of invivo human liver [C] // Proceedings of 12th Annual Meeting of International Society for Magnetic Resonance in Medicine, Tokyo, Japan, 2004: 502.

[10] Rouviere O, Yin M, Dresner M A, et al. In vivo MR elastography of the liver: preliminary results [C] // Proceedings of 13th Annual Meeting of International Society for Magnetic Resonance in Medicine, Florida, USA, 2005: 340.

[11] Dresner M A, Rose G H, Rossman P J, et al. Functional MR elastography of human skeletal muscle [C] // Proceedingsof 6th Annual Meeting of International Society for Magnetic Resonance in Medicine, Sydney, Australia, 1998: 463.

[12] Dresner M A, Rose G H, Rossman P J, et al. Magnetic resonance elastography of skeletal muscle [J]. Journal of Magnetic Resonance Imaging, 2001, 13: 269-276.

[13] Muthupillai R, Rossman P J, Greenleaf J F, et al. MRIvisualization of acoustic strain waves: effect of linear motion [C] // Proceedingsof 4th Annual Meeting of International Society for Magnetic Resonance in Medicine, New York, USA, 1996: 1515.

[14] Muthupillai R, Ehman RL. Amplitude modulated cyclic gradient waveforms: application in MR elastography [C] // Proceedings of 5th Annual Meeting of International Society Magnetic Resonance in Medicine, Columbia, Canada, 1997: 1904.

[15] Dunn T C, Majumdar S. Comparison of motion encoding waveforms for magnetic resonance elastography at 3T [C] // Conference of the IEEE Engineering in Medicine Biology Society, 2005, 7: 7405-7408.

[16] Uffmann K, Ladd M K. Actuation systems for MR elastography[J]. IEEE Engineering in Medicine and Biology Magazine 2008; 27: 28-34.

[17] Rossman P J, Muthupillai R, Ehman R L. Driver device for MR elastography [P]. 1999. US Pat.5952828.

[18] Talwalkar J A, Yin M, Fidler J L, et al. Magnetic resonance imaging of hepatic fibrosis: emerging clinical applications [J]. Hepatology, 2008, 47: 332-342.

[19] Kruse S A, Dresner M A, et al. MR elastography of human kidney in vivo: a feasibility study [C] // Proceedings of 12th Annual Meeting of International Society Magnetic Resonance in Medicine, Tokyo, Japan, 2004: 2600.

[20] Tse Z T H, Janssen H, Hamed A, et al. Magnetic resonance elastography hardware design: a survey [J]. Proceedings of the IMechE, Part H: Journal of Engineering in Medicine, 2009, 223:495-514.

[21] Manduca A, Smith J A, Muthupillai R, et al. Image analysistechniques for magnetic resonance elastography [C] // Proceedings of 5th Annual Meeting ofInternational Society Magnetic Resonance in Medicine, Columbia, Canada, 1997: 1905.

[22] Jenkinson M. Fast, automated, N-Dimensional phaseunwrapping algorithm [J]. Magnetic Resonance in Medicine, 2003,49: 193-197.

[23] Knutsson H, Westin C J, Granlund G. Local multiscale frequency and bandwidth estimation [C] // Proceedings of the IEEE International Conference on Image Processing, 1994, 1: 36-40.

[24] Manduca A, Muthupillai R, Rossman P J, et al. Local wavelength estimation for magnetic resonance elastography [C] // Proceedings of the International Conference on IEEE, 1996, 3: 527-530.

[25] Kruse S A, Smith J A, Lawrence A J, et al. Tissue characterization using magnetic resonance elastography: preliminary results [J]. Physics in Medicine Biology, 2000, 45: 1579-1590.